

# Phys Enph 479/879 Assignment #2: Extreme Nonlinear Optics: Dynamics of Coupled ODEs

Josh Dykstra<sup>1,\*</sup>

<sup>1</sup>*Department of Physics, Engineering Physics and Astronomy,  
Queen's University, Kingston, ON K7L 3N6, Canada*

(Dated: October 1, 2020)

This assignment introduces quantum two leveled systems and Rabi field interaction with and without the rotating wave approximation. It discusses the use of numeric ordinary differential equation solvers, including the likes of Euler's method and the Runge-Kutta family. Time dependent Gaussian pulses are manipulated and tuned to measure and test optical phenomena within the quantum two level system.

## I. INTRODUCTION

includes the rotating wave approximation and a constant Rabi field:

## II. THEORY AND EQUATIONS

### A. Two Level Systems and Rabi Oscillations

A two level system is a two dimensional quantum framework which is described by two states of the Hamiltonian's energy levels, the simplest quantum system possible. The system can exist in a superposition of the two states and under perturbation or a oscillatory driving field the system will cycle between the two states. This cycle is called a Rabi cycle, it describes the populations of the quantum levels and the periodic changes between absorption and stimulated emission of photons. A Rabi cycle can be modelled using the Optical Bloch Equations.

### B. Rotating Wave Approximation

The Rotating Wave Approximation (RWA) is an approximation used in optics that simplifies the interactions between lasers and atoms. Typically RWA is modelled with a coherent laser light field with characteristic frequency  $\omega_L$  interacting with an atom described as a two state system with resonant frequency  $\omega_0$ .

The system will not respond when the frequency of the laser does not match the resonant frequency of the atom, fast oscillations in the rotating wave approximation are discarded because they differ from the detuning of the laser field 1, which is approximately zero. The rotating wave approximation only keeps the slowly varying parts of the interaction with the Hamiltonian, ignoring counter rotating wave terms.

$$\Delta_{0L} = \omega_0 - \omega_L. \quad (1)$$

### C. Coherent Optical Bloch Equations

The differential equations that will govern the system and describe the Rabi oscillations are the coherent optical bloch equations, defined as follows. In it's simplest form it

$$\frac{du}{dt} = -i\Delta_{0L}u + i\frac{\Omega_0}{2}(2n_e - 1), \quad (2a)$$

$$\frac{dn_e}{dt} = -\Omega_0 \text{Im}[u]. \quad (2b)$$

For a none constant, or time dependent Rabi field we can introduce the full rotating wave approximation bloch equation, complete with dephasing:

$$\frac{du}{dt} = -\gamma_d u - i\Delta_{0L}u + i\frac{\tilde{\Omega}(t)}{2}(2n_e - 1), \quad (3a)$$

$$\frac{dn_e}{dt} = -\tilde{\Omega}(t) \text{Im}[u]. \quad (3b)$$

### D. Full Wave Bloch Equations

With no RWA the full Optical Bloch equations are required to solve the full Rabi problem. It differs from the Coherent equations as the detuning is replaced with the resonant frequency of the atom.

$$\frac{du}{dt} = -\gamma_d u - i\omega_0 u + i\Omega(t)(2n_e - 1), \quad (4a)$$

$$\frac{dn_e}{dt} = -2\Omega(t) \text{Im}[u]. \quad (4b)$$

### E. Euler Method

The Euler method or the forward step Euler method is the most primitive numeric procedural method of solving ordinary differential equations. Euler's method is a first order method which means the Taylor series has been truncated down to its first order, containing only first derivatives of the solution.

$$y_{n+1} = y_n + hf(t_n, y_n). \quad (5)$$

---

\* 19jld1@queensu.ca

This equation describes the algorithm for finding an approximate solution to some differential equation. Initial conditions are required to limit the method, for example the starting position is required ( $y_0$ ) along with a step size  $h$ . The approximate solution will converge with the exact solution in the approximation limit  $h \rightarrow 0$ .

### F. Runge-Kutta Methods

Euler's method is the simplest form of numerical integration, but it is very inaccurate at large step sizes. The Runge-Kutta family is a series of iterative methods for producing approximate solutions to differential equations, like Euler, that provides a more practical approximation. Euler, only calculates a single slope per interval, but Runge-Kutta 4 (RK4) the fourth iterative method, calculates four different slopes per step and finds the next anticipated position as an average of the different slopes.

$$k_1 = hf(t_n, y_n), \quad (6a)$$

$$k_2 = hf(t_n + \frac{h}{2}, y_n + \frac{k_1}{2}), \quad (6b)$$

$$k_3 = hf(t_n + \frac{h}{2}, y_n + \frac{k_2}{2}), \quad (6c)$$

$$k_4 = hf(t_n + h, y_n + k_3). \quad (6d)$$

Where  $h$  is the step size,  $f(t_n, y_n)$  is the derivative of the solution at time  $t_n$ . These four components create the basis for the complete iterative function:

$$y_{n+1} = y_n + \frac{1}{6}(k_1 + 2k_2 + 2k_3 + k_4), \quad (7a)$$

$$t_{n+1} = t_n + h. \quad (7b)$$

We can call this function multiple times to create the approximate solution to the differential equation. By reducing the step size ( $h$ ) the approximation converges on the analytical solution.

## III. IMPLEMENTATION

### A. Implementing a Runge-Kutta Ordinary Differential Equation Solver

To solve more difficult problems we must first have a working differential equation solver. We know that the error of the Euler forward step method diverges from the exact solution for large step sizes. Thus we will use the more accurate Runge-Kutta 4 method which as discussed will produce a approximate solution much closer to the exact analytical solution. Implementing equations 5, 7 and 7 we can compare the two methods to prove the accuracy differences for varying step sizes and ultimately show that RK4 is the superior tool. Increasing the step size of the function from  $h = 0.001$  to  $h = 0.01$  in the constant wave

solution, will show that the Euler method diverges greatly from the exact solution proving its unsuitability for solving the Optical Bloch equations.

### B. Time Dependent Gaussian Pulse

With a working ODE solver, solving the we can now introduce a more interesting time dependent Gaussian pulse instead of the constant wave that will excite the system and have some effect on the populations of the two level system.

$$\tilde{\Omega}(t) \rightarrow \tilde{\Omega}_{Gauss}(t) = \Omega_0 \exp\left(\frac{-(t-5)^2}{t_p^2}\right), \quad (8)$$

This is the Gaussian pulse, of width  $t_p$  and offset of 5 normalised units. For this solution we only consider on-resonance excitation with no dephasing ( $\Delta_{0L} = \gamma_d = 0$ ), this changes the standard Bloch RWA equations to the following:

$$\frac{du}{dt} = i \frac{\tilde{\Omega}(t)}{2} (2n_e - 1), \quad (9a)$$

$$\frac{dn_e}{dt} = \tilde{\Omega}(t) \text{Im}[u]. \quad (9b)$$

If the pulse area is defined to be  $2\pi$  we can calculate the pulse width ( $t_p$ ) for constant  $\Omega_0$  as follows:

$$2\pi = \int_{-\infty}^{\infty} \tilde{\Omega}_{Gauss}(t) dt, \quad (10a)$$

$$t_p = \frac{2\pi}{\Omega_0 \sqrt{\pi}}. \quad (10b)$$

### C. Finite Detuning and Dephasing

The last problem was a solution to the RWA Bloch equations only considering on-resonant excitation with no dephasing. We can now introduce finite detuning ( $\Delta_{0L}$ ) an dephasing ( $\gamma_d$ ) separately varying them from  $0 \rightarrow \Omega_0$ . The populations in the excited state will vary depending on how close to the resonance the tuning is, from this we can plot a graph of the peak populations as the detuning and dephasing changes.

### D. Full Rabi Problem

The last problem is to introduce the full Rabi problem with no rotating wave approximation 4. In this case  $u$  is quickly varying and  $\Omega(t)$  is now a full wave Rabi field:

$$\Omega(t) \rightarrow \Omega_{Gauss}(t) = \Omega_0 \exp\left(\frac{-t^2}{t_p^2}\right) \sin(\omega_L t + \phi). \quad (11)$$

With a  $2\pi$  area pulse we can investigate what happens to  $u(t)$  and the populations for on-resonance excitations ( $\omega_0 = \omega_L$ ) for different frequencies, namely ( $\omega_L =$

$20\Omega_0, 10\Omega_0, 5\Omega_0, 2\Omega_0$ ) with our pulse width  $t_p = 1$ . To obtain a  $2\pi$  pulse we must first find  $\Omega_0$ .

$$2\pi = \int_{-\infty}^{\infty} \tilde{\Omega}_{Gauss}(t) dt, \quad (12a)$$

$$\Omega_0 \sqrt{\pi} = 2\pi, \quad (12b)$$

$$\Omega_0 = 2\sqrt{\pi}. \quad (12c)$$

We can now investigate what happens to the populations and real and imaginary parts of the solution if we change the area of the pulse width for the full Rabi field if we keep the resonance constant ( $\omega_L = 4\sqrt{\pi}$ ).

### E. Fourier Transformation

Using a fast Fourier transform (FFT) we can measure the frequency decomposition of the transmitted or reflected pulse through its power spectrum.

$$P(t) \propto \text{Re}[u(t)]. \quad (13)$$

From this we can obtain  $|P(\omega)|$  using the Fourier transform to extract the frequency domain. The polarization decay rate of  $\frac{0.4}{t_p}$ . For the same pulse widths as described before we perform the Fourier transform on the real component of  $u$  and plot the normalised solution on a log scale, limiting the x-axis frequency domain ( $\frac{\omega}{\omega_L}$ ) from 0 to 6. It is necessary to increase the simulation length to make sure the transients decay to zero over time, a maximum time of  $t = 50t_p$  is suggested.

Finally we can use the library package in scipy, odeint, to compare how our differential equation solver performs. Using more packages we can measure the time it takes for each ODE solver to run thus establishing the practicality of our method.

## IV. RESULTS

### V. DISCUSSION AND CONCLUSIONS

#### A. RK4 Euler Comparison

As evident by the plot, the RK4 method is superior to Euler, the exact solution has even been offset from the RK4 method so that it is visible. This shows an excellent agreement between the RK4 method and the exact solution. By increasing the step-size by a factor of 10, ( $h = 0.01$ ) 1 shows the Euler method diverging from the exact solution, whereas RK4 doesn't as much, proving RK4 is better suited for larger step-sizes as anticipated.

#### B. Time Dependent Gaussian Pulse

(2) Shows the imaginary part of the solution along with the population variation for the on-resonant excitation with no dephasing from the time dependant Gaussian pulse of area  $2\pi$ . It shows the population completely in the ground

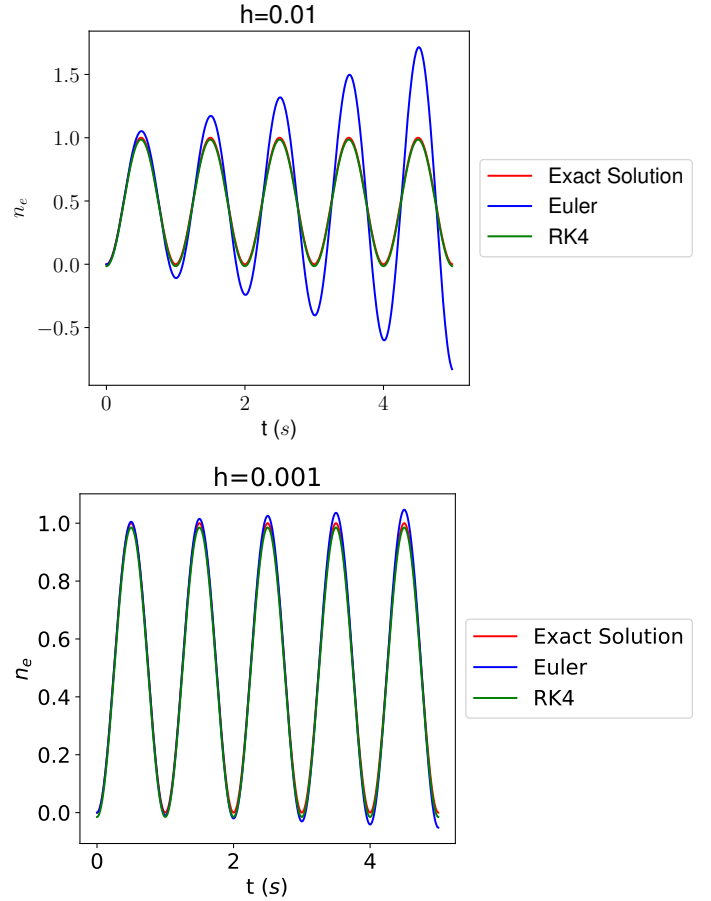


Figure 1. Plot showing the two different ODE solvers, Euler (Blue) against RK4 (Green) against the exact solution (Red) for different step sizes ( $h = 0.01$  Top,  $h = 0.001$  Bottom). Note, the exact solution has been displaced slightly to distinguish it from the RK4 method

state and as the excitation occurs all the atoms quickly become excited and move into the higher energy state before returning back to the ground state. This interaction takes 2 seconds from start to finish.

#### C. Detuning and Dephasing

The detuning figure (3) shows that as the frequency of the Rabi field ( $\omega_L$ ) deviates from the resonant frequency ( $\omega_0$ ) the maximum population of atoms in the excited state decreases and tends to 20% at  $2\pi$ . This is as expected considering the amplification that occurs for on-frequency resonance, by detuning the frequency less amplification will occur and net less atoms in the ground state will be excited into the higher energy state resulting in a lower maximum population.

The dephasing figure (3) shows a similar style curve to the detuning although the overall effect is less substantial. Dephasing only reduces the maximum population to a minimum at 55% for  $\gamma_d = 2\pi$ . Dephasing is the structure which determines how long a system will maintain its coherence for, this graph suggests that as the dephasing increases, destructive interference increases reducing the amplifica-

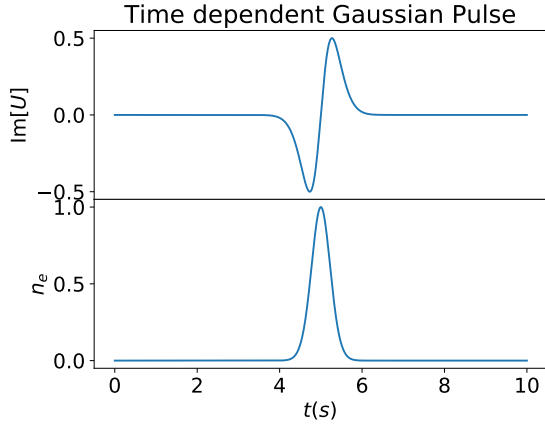


Figure 2. Time Dependent Gaussian Pulse of  $\Omega = 2\pi$ ,  $\gamma_d = 0$ . Plot offset by factor of 5 in normalised units.

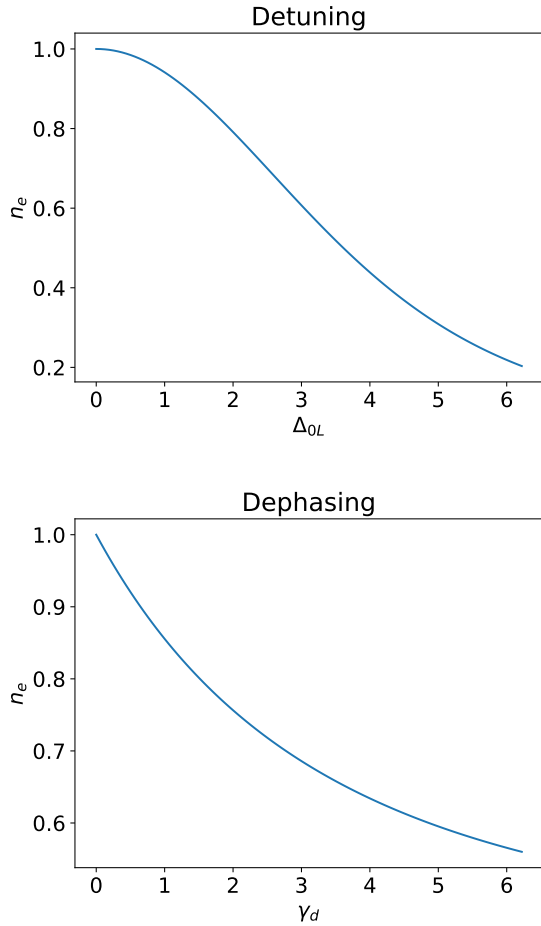


Figure 3. Graphs showing the maximum value for  $n_e$  for varying detuning or dephasing up to  $2\pi$ .

tion caused by the resonance and thus reducing again the maximum population of atoms in the excited state.

## D. Full Rabi Field

Introducing the full Rabi field the features of  $u(t)$  and  $n_e(t)$  can be studied. Figure (4) shows the solutions for fixed resonant frequencies:  $\omega_L = 20\Omega_0, 10\Omega_0, 5\Omega_0, 2\Omega_0$ . The rotating wave approximation is not possible here because the Gaussian pulse contains a slowly varying term which is a condition for RWA. Comparing these solutions to the rotating wave approximation it is evident that the same full excitation into the high energy state still occurs but at low frequency the smooth Gaussian like curve becomes distorted. The greater the frequency of the Rabi field the smoother the population excitation. The rotating wave approximation model cannot account for the phase of the drive because the sine term in the Full Rabi wave is too quickly varying which is ignored in the approximation, this does not make a difference to the solution.

Fixing the resonant frequency but varying the pulse area gives interesting results as seen in figures (6). It shows that the larger the area of the Gaussian pulse the more the randomness of the quantum fluctuations. The populations of the excited state deviates from the Gaussian curve into a more randomly spiked pattern, similar to the shape of Dirac delta functions as the area increases. Another effect of increasing the area is that the final population value is not the same, for an area of  $10\pi$  relaxation of the system does not occur and the system resides mostly in the excited state. The real and imaginary components of the solution show cyclic behaviour as the area increases after the Gaussian pulse has had its effect tending towards a harmonic solution after perturbation.

## E. Fourier Transform

Graph 7 shows, the Fourier transform of the real components of the solution which we have previously described as being the power spectrum decomposition. It shows the absolute value of the power as a function of frequency for varying pulse areas. Each spectrum shows the power of the system tending towards zero as the ratio  $\frac{\omega}{\omega_L}$  increases. As the pulse area increases the power distribution tends to zero at a higher frequency.

It also shows, in the last subplot, the Fourier transform of the ordinary differential equation library package solver for an pulse area of  $2\pi$ . This result matches the RK4 method's transform although the curve is not as smooth suggesting the step size used in the library package is larger than that used in the RK4 method. The times to compute the solutions were measured 10 times and the average was calculated as follows:

$$t_{scipy} = 0.006s \quad (14a)$$

$$t_{RK4} = 2.628s \quad (14b)$$

It's obvious from these times that the library package is better optimised than the RK4 method, but as said before it seems as if the step size is not the same which could suggest that it is not a fair test.

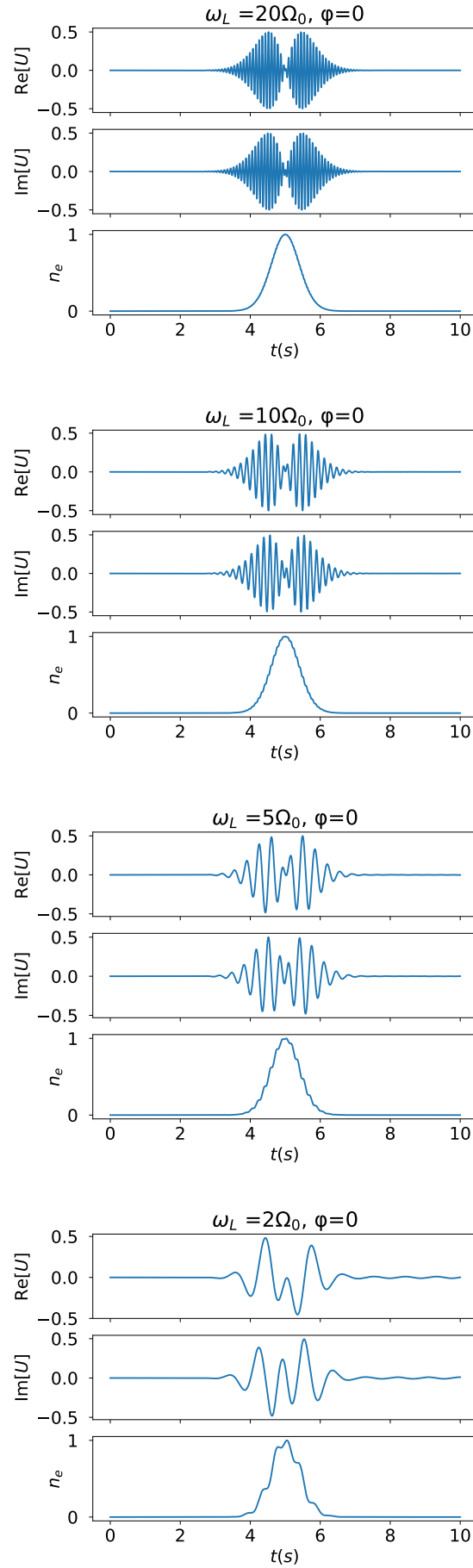


Figure 4. Graph showing the Imaginary, Real and Population ( $n_e$ ) values for  $u$  for fixed resonance and no phase difference.

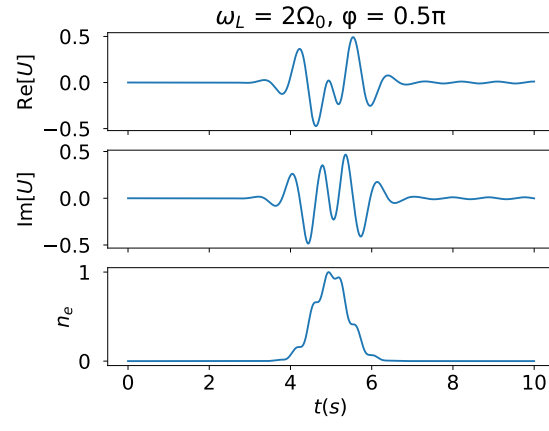


Figure 5. Populations, real and imaginary components of  $u$  for fixed resonance with phase difference.

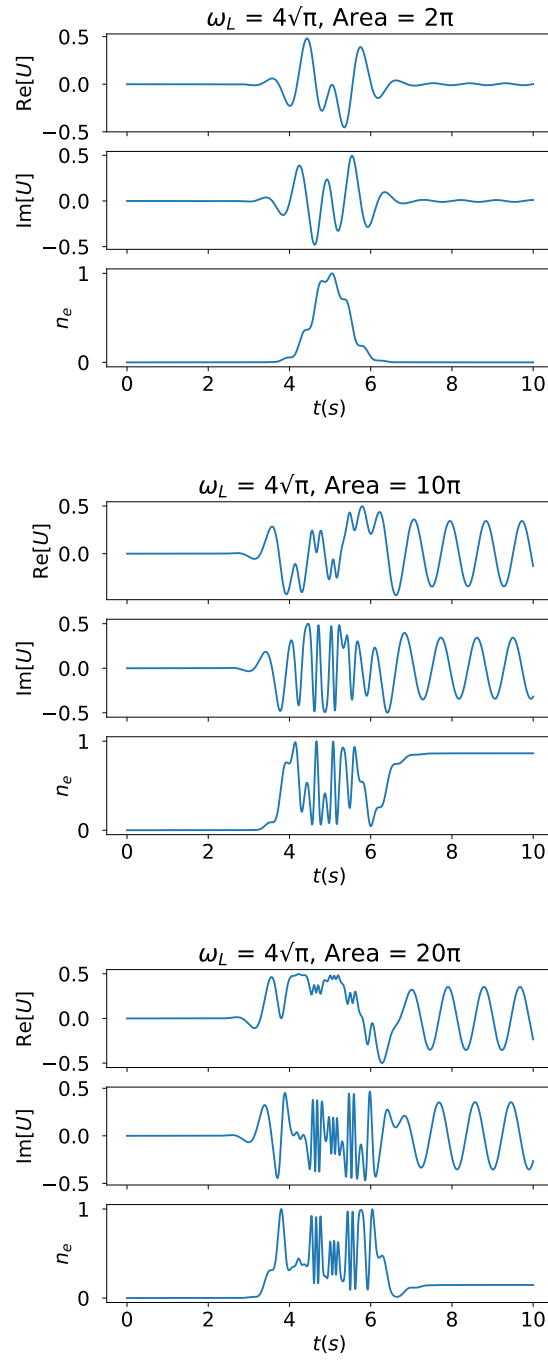


Figure 6. Imaginary, Real and Population ( $n_e$ ) values for  $u$ , with varying Gaussian pulse area with fixed resonance frequency.

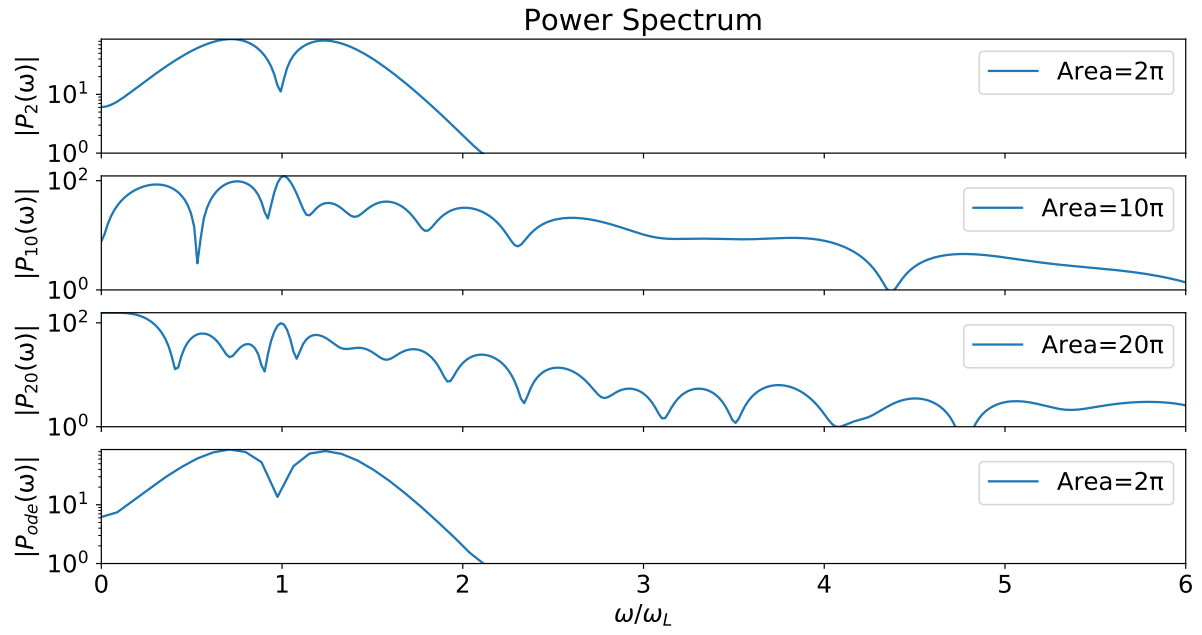


Figure 7. Graph showing the Fourier transform of the Real part of  $u$  for varying area. Also last plot is the Fourier transform of the